AFRRI TR89-1

AFRRI TECHNICAL REPORT

Laboratory x-ray irradiator for cellular radiobiology research studies: Dosimetry report

T. H. Mohaupt
G. H. Zeman
W. F. Blakely
M. M. Elkind

DEFENSE NUCLEAR AGENCY
ARMED FORCES RADIOBIOLOGY RESEARCH INSTITUTE
BETHESDA, MARYLAND 20814-5145

REVIEWED AND APPROVED

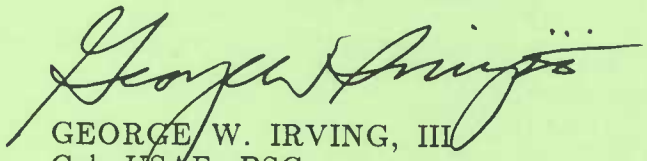

GEORGE W. IRVING, III
Col, USAF, BSC
Director

UNCLASSIFIED
SECURITY CLASSIFICATION OF THIS PAGE

REPORT DOCUMENTATION PAGE

1a. REPORT SECURITY CLASSIFICATION UNCLASSIFIED	1b. RESTRICTIVE MARKINGS
2a. SECURITY CLASSIFICATION AUTHORITY	3. DISTRIBUTION / AVAILABILITY OF REPORT Approved for public release; distribution unlimited.
2b. DECLASSIFICATION / DOWNGRADING SCHEDULE	
4. PERFORMING ORGANIZATION REPORT NUMBER(S) AFRRI TR89-1	5. MONITORING ORGANIZATION REPORT NUMBER(S)
6a. NAME OF PERFORMING ORGANIZATION Armed Forces Radiobiology Research Institute 6b. OFFICE SYMBOL (*If applicable*) AFRRI	7a. NAME OF MONITORING ORGANIZATION
6c. ADDRESS (*City, State, and ZIP Code*) Defense Nuclear Agency Bethesda, Maryland 20814-5145	7b. ADDRESS (*City, State, and ZIP Code*)
8a. NAME OF FUNDING / SPONSORING ORGANIZATION Defense Nuclear Agency 8b. OFFICE SYMBOL (*If applicable*) DNA	9. PROCUREMENT INSTRUMENT IDENTIFICATION NUMBER
8c. ADDRESS (*City, State, and ZIP Code*) Washington, DC 20305	10. SOURCE OF FUNDING NUMBERS PROGRAM ELEMENT NO.: IWED QAXM; PROJECT NO.; TASK NO.; WORK UNIT ACCESSION NO
11. TITLE (*Include Security Classification*) (see cover)	
12. PERSONAL AUTHOR(S) Mohaupt, [illegible] H.,[a] Blakely, W. F., Zeman, G. H.,[b] and Elkind, M. M.[c]	
13a. TYPE OF REPORT Technical 13b. TIME COVERED FROM _____ TO _____ 14. DATE OF REPORT (*Year, Month, Day*) 1989 April 15. PAGE COUNT 26	
16. SUPPLEMENTARY NOTATION	

17 COSATI CODES			18. SUBJECT TERMS (*Continue on reverse if necessary and identify by block number*)
FIELD	GROUP	SUB-GROUP	

19. ABSTRACT (*Continue on reverse if necessary and identify by block number*)

Dosimetry measurements were performed on a 50 kVp laboratory x-ray irradiator for cellular radiobiology research. The measurements were done with a parallel-plate ionization chamber, which had a thin aluminized-mylar window, and an extrapolation chamber. Intercomparison of dosimetry data from the two independent methods showed excellent agreement. Results are presented for radiation dose rate, uniformity, and beam quality for operation of the tungsten target, beryllium window x-ray tube at 50 kVp, 20 mA, and with filters either 0.012 mm, 0.180 mm, or 0.633 mm thick, for arrays positioned at a range of distances from the x-ray tube. The data in this report establish a dosimetric link between the cellular radiobiology research to be performed at AFRRI with the 50 kVp laboratory x-ray irradiator and the landmark work performed by Elkind and Sutton (1960) with a similar device.

20. DISTRIBUTION / AVAILABILITY OF ABSTRACT ☐ UNCLASSIFIED/UNLIMITED ☒ SAME AS RPT. ☐ DTIC USERS	21. ABSTRACT SECURITY CLASSIFICATION UNCLASSIFIED
22a. NAME OF RESPONSIBLE INDIVIDUAL Sylvia Saguiero	22b. TELEPHONE (*Include Area Code*) (202) 295-[illegible] 22c. OFFICE SYMBOL ISSP

DD FORM 1473, 84 MAR 83 APR edition may be used until exhausted
All other editions are obsolete

SECURITY CLASSIFICATION OF THIS PAGE
UNCLASSIFIED

12. Current addresses are as follows:

[a]Nuclear Medicine Department
Great Lakes Naval Hospital
Great Lakes, IL 60008-5237

[b]Radiation Protection Department
AT&T Bell Laboratories
600 Mountain Avenue
Murray Hill, NJ 07974-2070

[c]Department of Radiology and
Radiation Biology
Colorado State University
Ft. Collins, CO 80523

CONTENTS

INTRODUCTION

In 1985, the Armed Forces Radiobiology Research Institute (AFRRI) acquired a 60 kVp x-ray irradiator (figure 1) from Argonne National Laboratory, Argonne, IL, for cellular radiobiology experiments. This irradiator is similar to one used by Elkind and Sutton (1) for their landmark investigations. The shielding, space, and logistical requirements for the irradiator are minimal, allowing it to be conveniently located in a typical laboratory. Because of its simplicity of operation and inherent safety mechanisms, an investigator or technician can qualify easily to use the radiation source independently.

This report describes the dosimetry methods used to calibrate the beams planned for cell irradiations. Measurements of exposure rate, beam quality, and field uniformity were made with a thin-window, parallel-plate ionization chamber. Elkind and Sutton (1) used a variable-volume extrapolation chamber to provide dosimetry for their irradiator because of its excellent capability of measuring low-energy photons. We had the good fortune to use Elkind's variable-volume extrapolation chamber for comparison with the parallel-plate chamber. Comparison of the dosimetry data showed very good agreement between results obtained by the two methods.

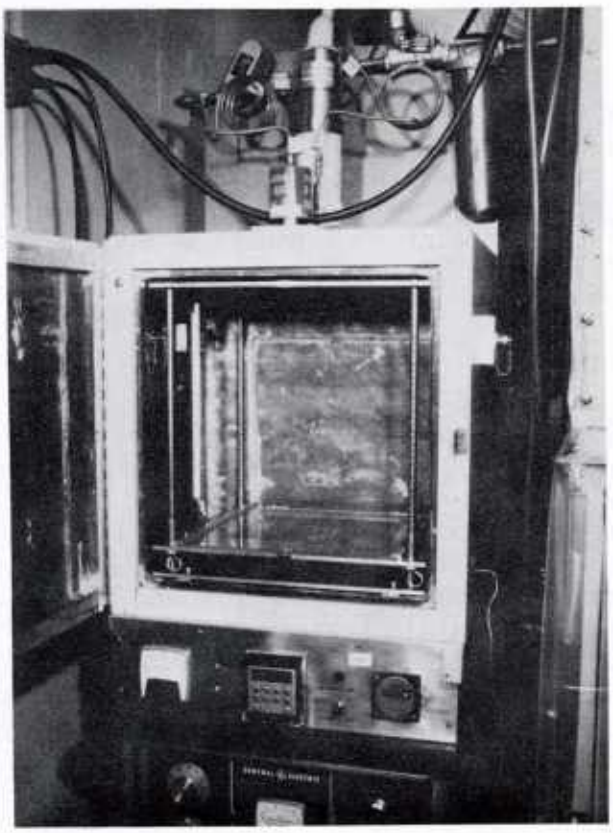

Figure 1. AFRRI laboratory irradiator for cellular radiobiology.

MATERIALS AND METHODS

Irradiator

The x-ray irradiator consists of a x-ray machine (Model No. DXE-225, General Electric Company, Milwaukee, WI), a x-ray tube (Model No. OEG-60, Machlett Laboratories Inc, Stamford, CT), and a shielded cabinet. The x-ray machine operated at peak voltages and currents of up to 60 kVp and 25 mA, respectively. The tube head is water-cooled for continuous operation. The tungsten target angle is 45 degrees to minimize anode heel effects. The tube window has an inherent filtration of 1.5 mm of beryllium (Be), which allows passage of a significant portion of the low-energy x rays. The irradiation time is controlled by a microprocessor-based solid-state timer (Model CX300, Eagle Signal Industrial Controls, Davenport, WI).

The irradiation cabinet has interior dimensions of 56 cm by 42 cm by 45 cm. The inner walls (including the door, top, and bottom) are lined with 2 mm of lead for effective personnel protection. A plastic shelf inside the chamber provides a stable, highly repeatable platform for experimental dosimetry devices and cell samples. The shelf is movable in the vertical (Z) axis by increments of 1 cm. The Z axis is at the center of crossed lines etched into the plastic shelf.

Radiation surveys at the exterior surface of the irradiator during operation at maximum power have shown no radiologic hazard due to beam leakage, thereby permitting experimental preparations to proceed in the lab during irradiation. The only detectable response was 0.5 mrem/hour on contact with the x-ray tube. At 10 cm from the tube, this response was negligible. As a precaution, two safety lights (and an audible alarm, if activated) alert occupants in the laboratory when x rays are being generated. Also, an interlock mechanism prevents the machine from working when the cabinet door is open and automatically turns the irradiator off when the door is opened during operation.

Beam Filtration

Aluminum (Al) filters were added at the exit port of the Be window to increase the effective energy of the x-ray beam by removing many of the low-energy x rays (2). Three thicknesses of Al (that is, 0.633 mm, 0.180 mm, and 0.012 mm) were used for all dosimetric measurements. The tube voltage and current used were 50 kVp and 20 mA, respectively. The 0.633-mm Al filter was used for intercomparison measurements because it simulates a field at the National Institute of Standards and Technology (NIST), Gaithersburg, Maryland, and was used to calibrate the parallel-plate ion chamber. The 0.180-mm Al filter is comparable to that used by Elkind (1). The 0.012-mm Al filter provides negligible filtration of low-energy x rays, hence, it offers a higher dose rate.

Culture Dish Arrays

Typically, cells are maintained in tissue culture petri dishes under monolayer growth conditions bathed in nutrient media to a depth of about 3 to 5 mm (approximately 5 ml per 60-mm-diameter dish or 20 ml per 100-mm-diameter dish). The petri dish is capped with a plastic cover approximately 1 mm thick, which assists both to maintain sterility and to decrease evaporative loss of media.

The x-ray energy spectrum produced at a peak voltage of 50 kV and with added Al filters readily undergoes attenuation by the plastic tissue-culture petri dish covers or the culture media. For example, using a beam hardened with 0.180 mm of Al the attenuation due to the medium can be as high as 60%, and the plastic cover will reduce the beam an additional 15%. Further, inconsistencies in the thickness of medium above the cells can result in large changes in the x-ray energy spectra reaching the cells. To avoid these problems, Elkind and Sutton (1) irradiated cells with a minimum of absorbing material between the radiation source and biological target. An ultra-thin cover of plastic wrap (Saran) secured in a plastic ring with brass screws substitutes for the petri dish cover during irradiations and decreases the possibility of contamination without severely diminishing the photon fluence. Further, all excess culture media was aspirated from the petri dish, leaving the cells without a significant media-induced shielding during irradiation.

Reproducibility of the positioning of the biological target material relative to the radiation source was accomplished in the following manner. Either 60-mm or 100-mm-diameter tissue-culture petri dishes were placed on the plastic tray in custom acrylic holders to provide several arrays for irradiation (figure 2). The petri dish array was centered on the Z axis of the irradiator by a centering plate. Cell cultures can be irradiated at room temperature or at the temperature of ice water. For ice water irradiations, an adaptor raises the large petri dish by 1 cm for ice water to be placed beneath the cell plate, thereby facilitating a common vertical scale (3).

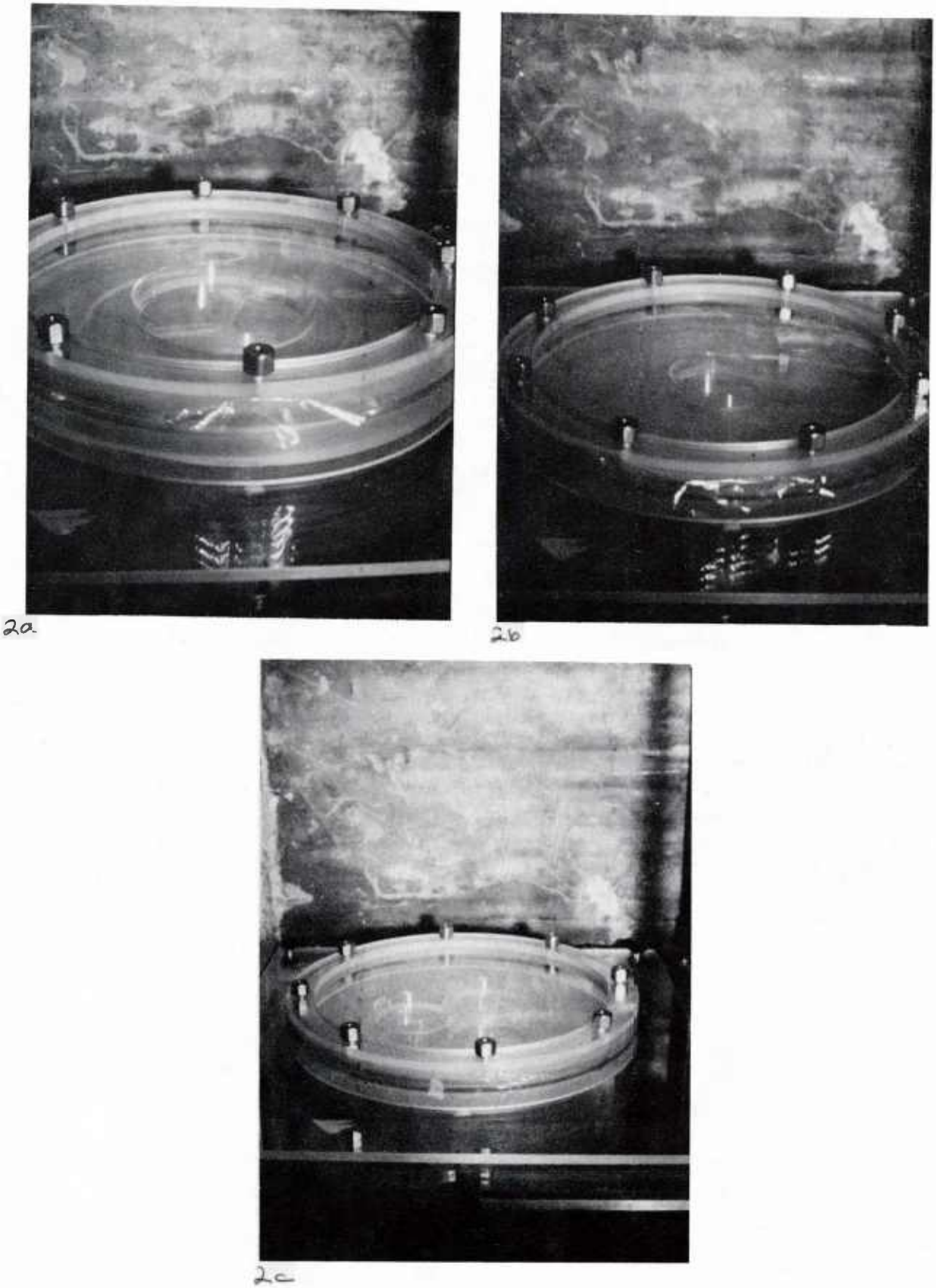

Figure 2. Culture dish arrays: a. 100-mm diameter; b. 60-mm diameter; c. 60-mm diameter in three dish array.

Parallel-Plate Ionization Chamber

A parallel-plate ionization chamber made by Capintec, Inc. (Model No. PS-033, Pittsburg, PA) was used to measure the exposure rate. Its thin window has a thickness of 0.5 mg/cm^2 of aluminized mylar, and its sensitive volume is 0.5 cm^3. The detector body is made of polystyrene. The chamber was calibrated at NIST with two x-ray fields (table 1) (4). Appendix A shows the NIST energy spectrum for the unshielded, 20 kVp calibration field and an energy spectrum with irradiation parameters similar to the NIST L50 x-ray field (5). The difference between the calibration factors for the two beams was 2.4%. This indicated that the chamber response changed minimally over a range of low energies. Charge accumulation was made with a Keithley Model 616 digital electrometer (Cleveland, OH) for the duration of exposure. Collecting charge was the appropriate method of ionization measurement because this is the mode used by NIST to calibrate the chamber. The half-value layer (HVL) is the thickness of material required to reduce an x-ray beam to half its original intensity. The homogeneity coefficient is simply the ratio of the first and second HVL's. Appendix B shows the method of calculation for exposure and dose rates.

Preliminary measurements on the x-ray irradiator indicated that the parallel-plate chamber showed negligible ion recombination characteristics and polarity differences. Readings taken over several days at the same position showed a precision of ±1.5%.

Table 1. NIST Calibration Parameters of Parallel-Plate Chamber

NIST field	kVp	Added filter (mm Al)	HVL (mm Al)	Homogeneity coefficient	Calibration factor (R/nC)
L20	20	None	.071	.76	6.349
L50	50	.639	.75	.58	6.502

Elkind Variable-Volume Extrapolation Chamber

An extrapolation chamber is an ionization chamber in which the sensitive volume may be accurately changed by varying the separation distance between the window and collecting plate. It is a fundamental method of measuring exposure rate so that instrument calibration is unnecessary (6). Appendix C shows the derivation of the equations used to compute exposure rate from extrapolation chamber measurements. The extrapolation chamber (figure 3) used for comparison with the parallel-plate chamber is a custom device provided by Dr. M. M. Elkind. The chamber has a 50-μm-thick Be window (1) and a dual anode with collecting surface diameters of 1 cm and 4 cm. The potential difference applied to the collecting plate was -1,500 volts per centimeter with respect to the Be window. The collected current was read on the same electrometer as used with the parallel-plate chamber. (The difference between the electrometer current (nA) and charge (nC/sec) modes was measured to be 1.6% with a Keithley 261 Picoampere source in conjunction with a Hewlett-Packard 85 computer and 3421A Data Acquisition/Control Unit (Corvallis, OR).)

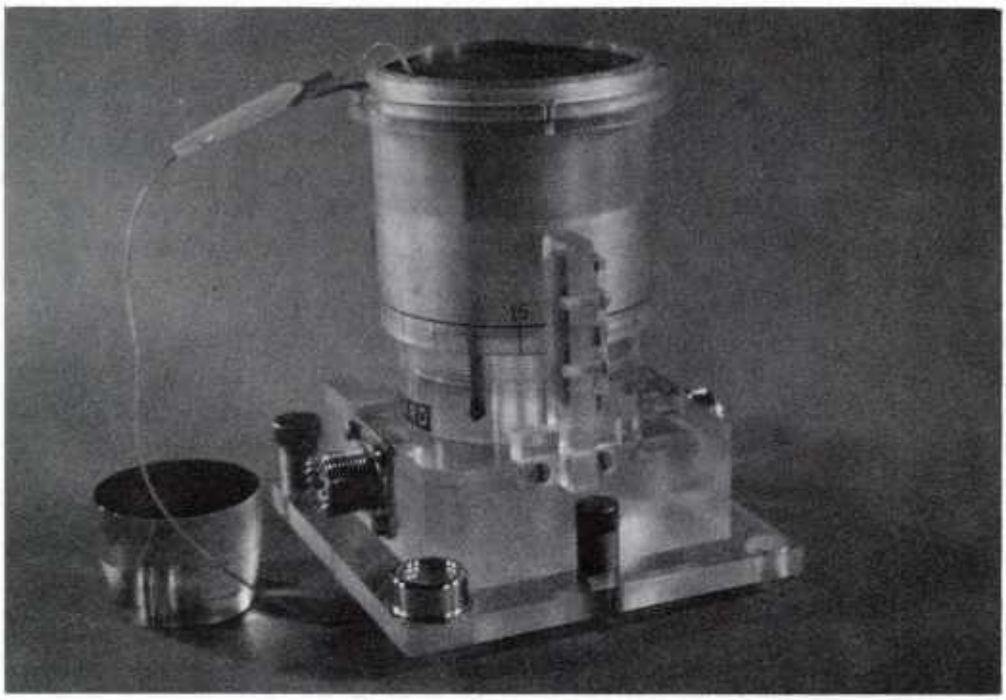

Figure 3. Elkind's extrapolation chamber with collecting plate.

RESULTS

Tube Potential and Timer Accuracy

Peak tube potential and quality assurance measurements for timer accuracy were made with a Mini-X kVp/Timer Meter (RTI Electronics Lab, AB, Sweden). The Mini-X was capable of accurately measuring x-ray tube voltage down to 44 kVp and timer accuracy for times up to 20 seconds. The measured value of kVp from the Mini-X agreed with the x-ray generator settings of 50 kVp and 55 kVp to within +/- 1% and at 45 kVp to within 3.5%. The x-ray timer setting was consistently 2% higher than the time measured by the Mini-X. This difference is due partly to the fact that the x-ray timer indicated the full exposure time while the Mini-X displayed the time that the exposure rate exceeded 75% of the maximum. To further evaluate the timer accuracy, charge was collected by the parallel-plate chamber over a range of exposure times for each beam quality (figure 4). The slopes of the fitted values have units of nC/sec. Comparison of each slope with the measured current shows an overresponse of the charge readings relative to the current readings by an average of 1.5%. This agrees with measurements taken with the picoampere source. The intersection of each line with the time axis shows negligible offset from the origin.

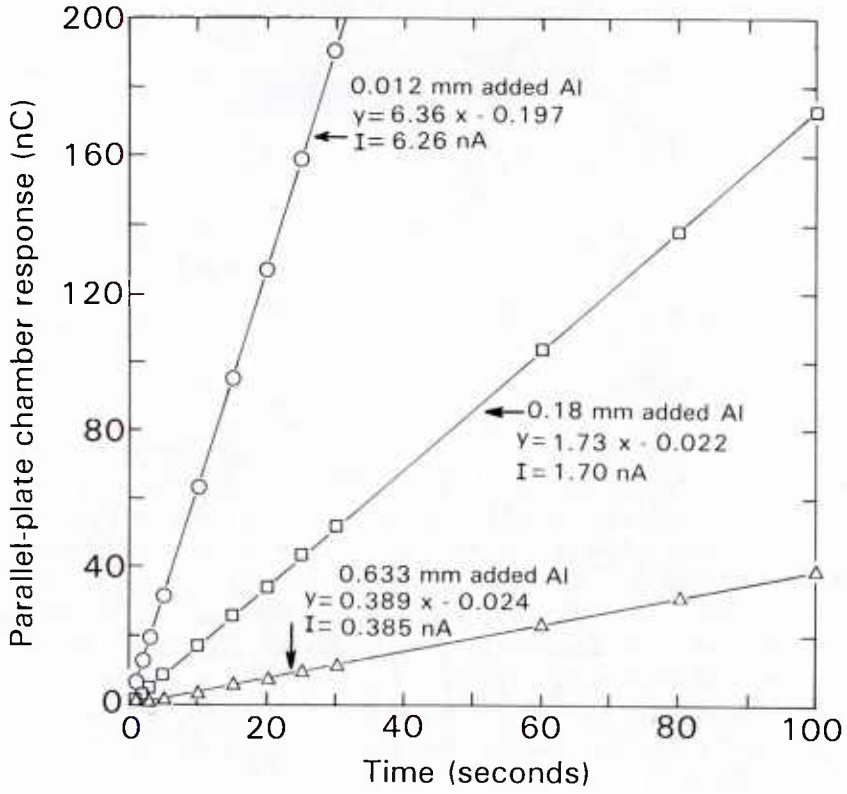

Figure 4. X-ray timer evaluation.

Focal Spot Measurements

The focal spot is the area on the target that accelerated electrons strike to produce x rays, and it correlates to the effective source size. The focal spot image of the irradiator was recorded on radiographic film through a pinhole aperture of 0.2 mm in a sheet of 1.6-mm lead placed midway between the source and the film. The size of the effective focal spot was calculated to be 6 mm by 7 mm using a similar triangles technique (7). Figure 5 shows an enlargement of the focal spot radiographic image.

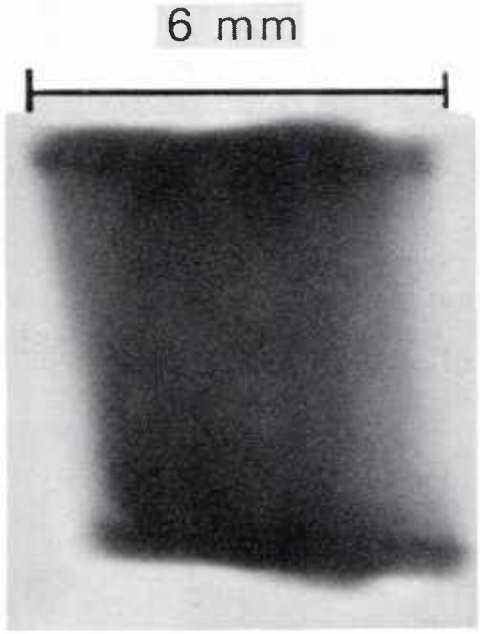

Figure 5. Enlargement of focal spot image.

Beam Quality

When an energy spectrum of an x-ray beam is not available, its penetrability or quality is described in terms of its HVL. The material of choice for measuring beam quality of this irradiator is Al. Because of the space limitation inside the irradiator chamber, ideal conditions for measuring HVL's as described by Trout (8) could not be attained. To approximate the ideal conditions, the distance between the source and the parallel-plate chamber was 36.8 cm with the filter placed halfway between. A collimator arrangement (figure 6) restricted the beam to the chamber's window. Table 2 shows beam quality data for several thicknesses of added Al at 50 kVp and no added Al at 20 kVp. The approximate equivalent photon energy for each beam's HVL was referenced from Johns and Cunningham (7).

Figure 6. Collimator arrangement used for half-value layer measurements.

Table 2. Parameters of Beam Quality

kVp	Added filter (mm Al)	HVL (mm Al)	Homogeneity coefficient	Approximate equivalent energy (keV)
20	none	0.058	0.80	8
50	.012	.077	.70	9
50	.18	.16	.37	10
50	.333	.53	.33	19

The measured HVL values for the 20 kVp and 50 kVp/0.633 mm Al measurements are significantly lower than the respective NIST L20 and L50 HVL values shown in table 1. The differences, which indicate the AFRRI x-ray unit has a softer energy spectra, are likely due to the various ways the tube potential is supplied. The NIST power supply is constant potential whereas the laboratory x-ray irradiator potential is half-wave rectified single phase.

Parallel-plate Window Transmission

The ability of the parallel-plate chamber to transmit low-energy photons through the aluminized mylar window was tested by measuring x-ray transmission through mylar. The HVL of mylar for two different x-ray beams was measured with the collimator system. The two beams were 50 kVp with 0.633 mm of added Al and 20 kVp with no added filtration. The measured HVL's were 876 and 94.4 mg/cm^2 for the 50 kVp and 20 kVp beams, respectively. The calculated attenuation due to the chamber window is 0.04% and 0.30% for each of the respective beams. This method provided an approximation because the mylar attenuators were not aluminized.

Intercomparison

Intercomparison between the parallel-plate ionization chamber and the extrapolation chamber was made with AFRRI's laboratory x-ray irradiator to verify the parallel-plate chamber's ability to measure low-energy exposures. The parameters measured were (a) exposure rate, (b) falloff with increasing vertical (Z axis) distance, (c) falloff in field size (X-Y axes), and (d) output charges with current and voltage. The amount of added filtration used was 0.633 mm of Al. Unless altered for experimental purposes, the tube voltage, current, and source-to-detector distance (SDD) were set at 50 kVp, 20 mA, and 19.2 cm, respectively.

Comparison of Exposure Rates

Ionization current measurements were made while changing the distance separating window and collecting plate of the extrapolation chamber. These measurements were repeated for both of the available plate collecting diameters on Elkind's extrapolation chamber. The results of these measurements are presented in figure 7. The slope of the fitted line for each set of measurements, when applied to equation 1 of appendix D, resulted in the exposure rate at the midpoint of the chamber. The intercepts of the extrapolated lines on the abscissa fell at about 0.09 cm.

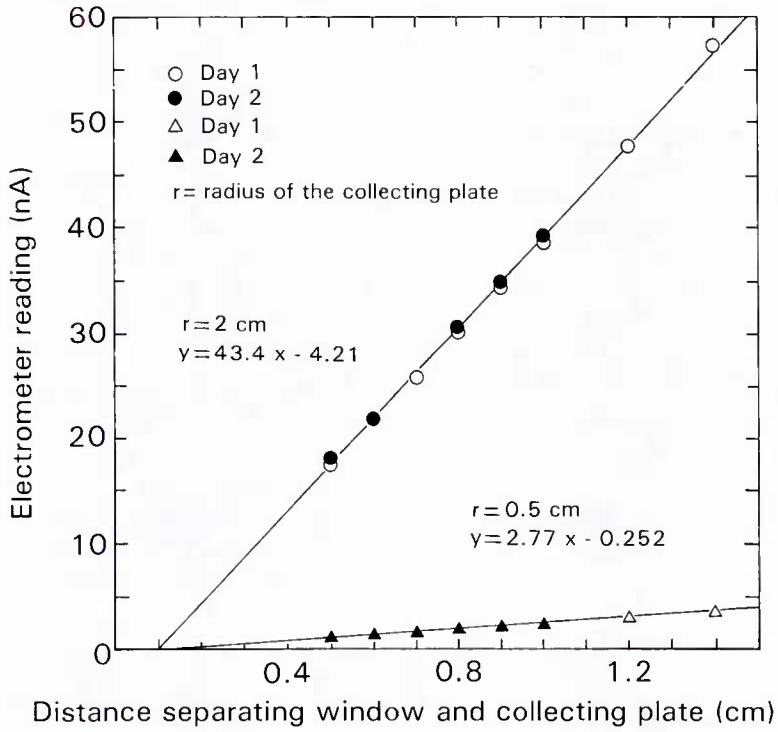

Figure 7. Effect of changing volume on extrapolation chamber.

Table 3 shows the values used to evaluate the exposure rate. The average exposure rate of the four extrapolation measurements was 10.5 R/sec, with a standard deviation representing 1.6% of the mean. The exposure rate as measured by the parallel-plate chamber was 10.6 R/sec. The method used to calculate the exposure rate to the parallel-plate chamber is equation 1 in appendix B. The excellent agreement between these two methods establishes a link between the landmark radiobiology experiments of Elkind and colleagues at the Argonne National Laboratory and those performed with the new unit at AFRRI.

Table 3. Exposure Rate Evaluation of Extrapolation Chamber and Parallel-Plate Chamber

Chamber*	Day	Diameter (cm)	Temperature (C^{o})	P (mm Hg)	Slope ($\Delta A/\Delta h$)	X intercept (cm)	X (R/sec)
EC	1	4	22.6	753.8	43.8	0.107	10.6
EC	1	1	22.6	753.8	2.78	.093	10.7
EC	2	4	23.1	757.0	42.7	.081	10.3
EC	2	1	23.1	757.0	2.74	.083	10.5
PPC	NA	NA	NA	NA	NA	NA	10.6

*EC = extrapolation chamber; PPC = parallel-plate chamber.

Inverse Square Measurements

The measurement of beam falloff with increasing distance from the source was made with the parallel-plate and extrapolation (4-cm diameter only) chambers. Figure 8 shows the ratio of the observed to expected values at successive distances from the source. The point of normalization was 19.2 cm from the source. After 16 cm, the falloff of both chambers yielded an inverse square relationship to within 1%. Additional measurements were made by the parallel-plate chamber along the same axis with added filters of 0.180 mm and 0.012 mm Al. Figure 8 compares these data and shows that filtration with thinner filters caused greater deviation from the inverse square law. This was the expected result because air acted as an effective attenuator for the low-energy x rays transmitted through the thin filters. The slopes of the two lines were approximately 0.006 cm^{-1}, which was consistent with the linear attenuation coefficient for 10 keV x rays in air (7).

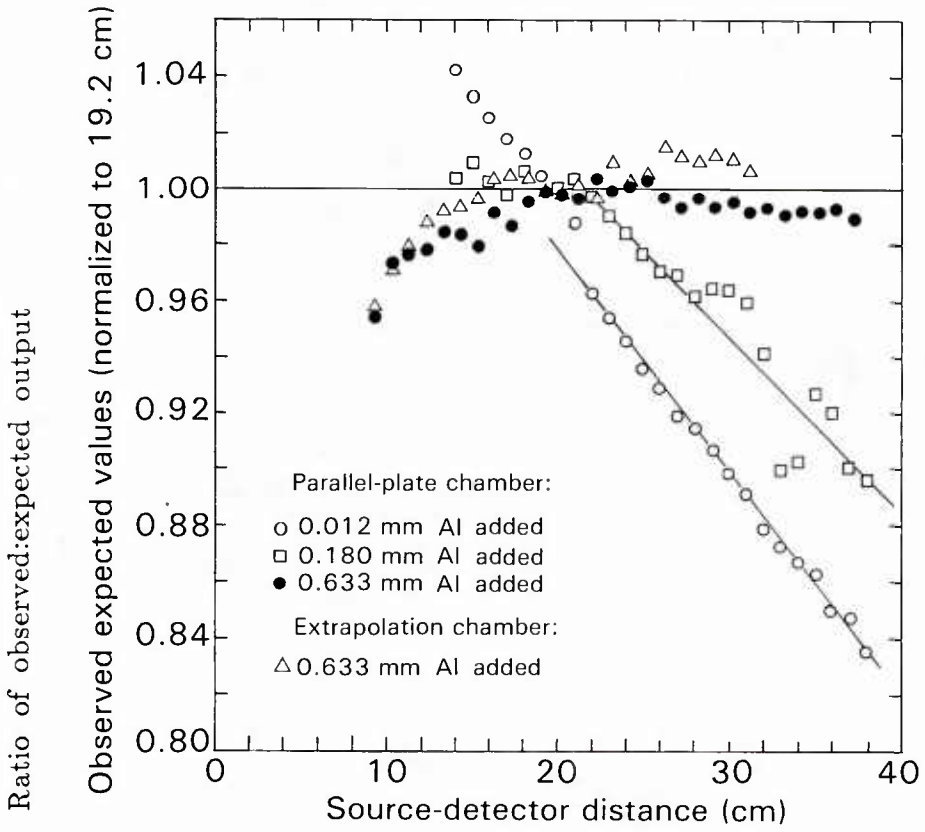

Figure 8. Radiation output measurements normalized to expected values. Expected values were calculated using the inverse square law referenced to the output at 19.2 cm distance.

Beam Falloff in the X-Y Plane

Beam intensity measurements in the horizontal plane at 19.2 cm were made with the parallel-plate and extrapolation (4-cm diameter only) chambers. The measurements were made diverging from the geometrical center toward the front, back, left, and right. The values were normalized to the geometrical center. Figure 9 shows field distribution was in excellent agreement between the parallel-plate chamber and 4-cm-diameter extrapolation chamber. The center of the field was at the geometrical center of the beam for both chambers. The diameters of the fields for 95%, 92.5%, and 90% uniformity are 4.7 cm, 6.3 cm, and 7.3 cm, respectively.

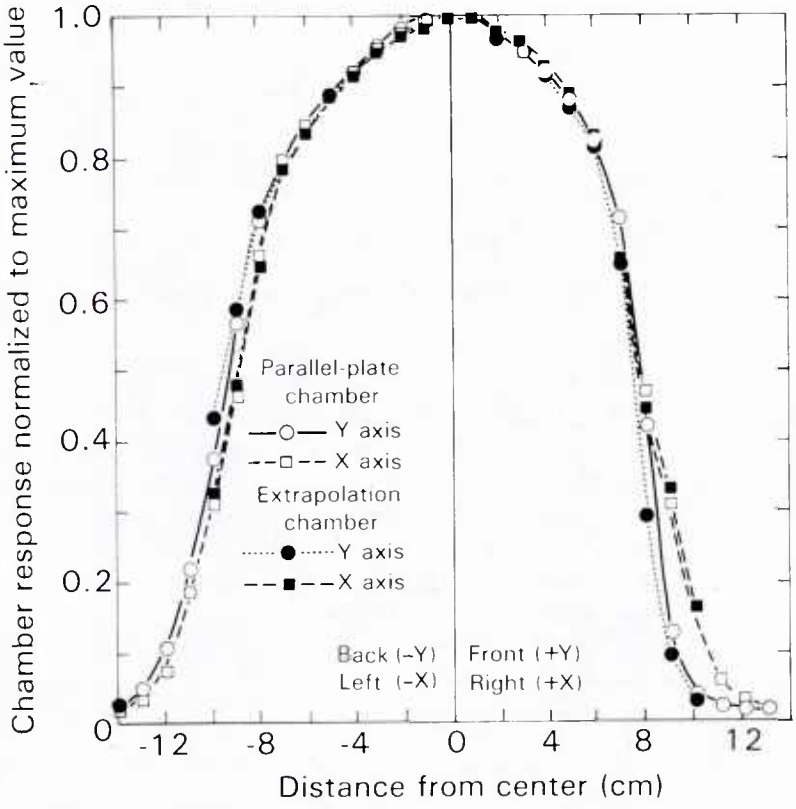

Figure 9. Intercomparison of field uniformity measurements.

Tube Current and Voltage

The linearity of the x-ray output with tube current over a range of 8 mA to 25 mA was evaluated by the parallel-plate chamber and both collection plate diameters of the extrapolation chamber. Figure 10 shows the tube current dependence of each ionization chamber's response as normalized to its sensitive volume. The results show excellent agreement and linearity over the entire range of x-ray tube current.

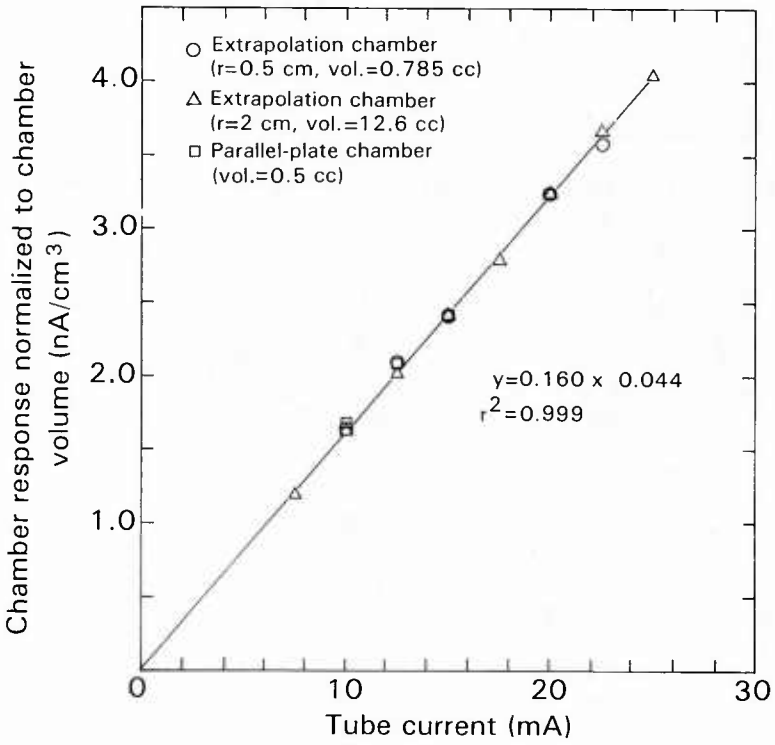

Figure 10. Linearity of x-ray output with tube current.

Figure 11 shows the effect of varying tube voltage on each chamber's volume-normalized response. Agreement between the two anode diameters of the extrapolation chamber was quite good. Agreement of the parallel-plate chamber was also good at lower voltages, but shows an overresponse at higher voltages, which peak at 5% at 50 kVp. The data in figure 11 were fitted with both linear and power function curves, as shown. Both the linear and power function correlation coefficients were greater than 0.995.

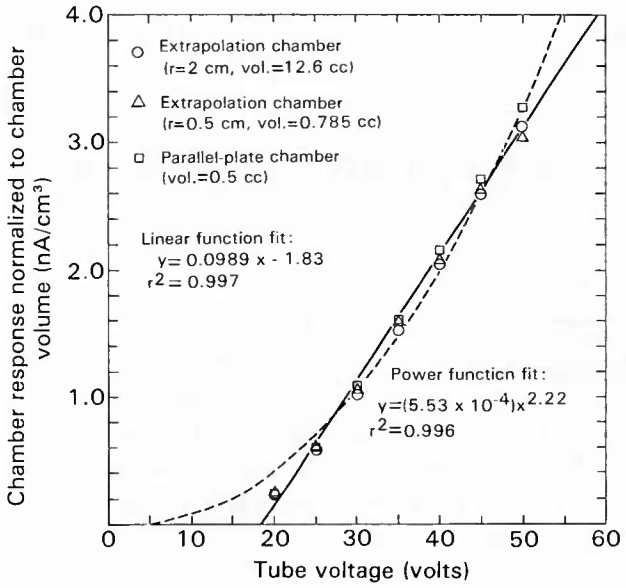

Figure 11. X-ray output as a function of tube voltage.

Dosimetry Measurements

The cellular dose was calculated from parallel-plate measurements taken along the Z axis for three beam parameters. The beam parameters were 50 kVp with added filtration of 0.633 mm, 0.180 mm, and 0.012 mm Al. Equation 2 of appendix B shows the method of dose calculation. Tables 4-6 show the dose rate at incremental distances from the source at the geometrical center for the single-plate arrays. The hole number is the position where the plate was placed to attain the respective source-to-cell distance. One shelf height was for the room temperature setup and the other was for the ice water setup. The uniformity measurements at each distance were derived from falloff measurements in the X-Y plane at several Z-axis positions for each beam. From those measurements, cones of uniformity were constructed to ensure 90%, 92.5%, and 95% uniformity across the plate. Thus, an investigator can use the dose rate and uniformity that best suits the experimental needs.

While taking beam profile measurements with the thinner filters, we observed that the point of maximum beam intensity was offset from the vertical axis towards the back of the cabinet (-Y direction). This effect was enhanced at greater source-to-detector distance (SDD). The displacement for the 0.180-mm Al beam was 0.3 cm at 15 cm SDD and increased to 1 cm at 40 cm SDD. The displacement of the 0.012-mm Al beam was 0.5 cm at 15 cm SDD and increased to about 2 cm at 40 cm SDD. While this effect was not fully characterized, it probably resulted from a variation in the x-ray energy spectrum across the x-ray beam in the direction of the anode-cathode axis. Because the offset varied with both the SDD and added filtration, the irradiation arrays were left in place at the X-Y plane origin. As a result, the cone of uniformity was slightly narrower than if it had been centered at the point of peak intensity. In the worst case, the deviation of the maximal intensity from the intensity at the geometric axis was 0.5%.

Incomplete aspiration of culture medium from the petri dishes before irradiation can markedly influence the uniformity of cellular x-ray dosage. This was demonstrated by the results of a pilot experiment on x-ray dose response and cell survival that used the 0.012 mm Al filter. An anomalous cluster of cell colonies around the periphery of the culture plate was observed in the high radiation dose samples. Investigation into this abnormality suggested that this effect was produced by the shielding of x rays by a meniscus of excess culture fluid that was created by not aspirating all of the excess cell culture medium from the petri dish. This was confirmed by repeating the experiment with complete medium aspiration (that is, all of the excess medium was removed), which resulted in the elimination of the ring of colonies. Upon the addition of incremental amounts of medium, the medium-induced shielding around the outer edge reappeared. Figure 12 shows cell survival populations after staining when the culture medium had been aspirated completely, followed by the addition of

Table 4. Dose Rate Chart of 0.633-mm Al Beam

Hole # Room temp	Hole # Ice water	Shelf height SDD (cm)	Dose rate (cGy/s)	Uniformity of cell irradiation (percentage) 60-mm dish	100-mm dish	Array of 3 60-mm dishes
9	10	15.3	14.6	92.5	NA	NA
10	11	16.3	12.8	92.5	NA	NA
11	12	17.3	11.4	95	NA	NA
12	13	18.3	10.2	95	NA	NA
13	14	19.3	9.17	95	90	NA
14	15	20.3	8.29	95	90	NA
15	16	21.3	7.53	95	92.5	NA
16	17	22.3	6.87	95	92.5	NA
17	18	23.3	6.29	95	92.5	NA
18	19	24.3	5.87	95	92.5	NA
19	20	25.3	5.33	95	92.5	NA
20	21	26.3	4.94	95	92.5	NA
21	22	27.3	4.58	95	92.5	90
22	23	28.3	4.26	95	95	90
23	24	29.3	3.98	95	95	90
24	25	30.3	3.72	95	95	90
25	26	31.3	3.48	95	95	92.5
26	27	32.3	3.27	95	95	92.5
27	28	33.3	3.08	95	95	92.5
28	29	34.3	2.90	95	95	92.5
29	30	35.3	2.74	95	95	92.5
30	31	36.3	2.59	95	95	92.5
31	32	37.3	2.45	95	95	92.5
32	33	38.3	2.33	95	95	92.5
33	34	39.3	2.21	95	95	92.5
34	35	40.3	2.10	95	95	92.5
35	36	41.3	2.00	95	95	92.5
36	37	42.3	1.91	95	95	92.5
37	NA	43.3	1.82	95	95	95

Table 5. Dose Rate Chart of 0.180-mm Al Beam

Hole # Room temp	Hole # Ice water	Shelf height SDD (cm)	Dose rate (cGy/s)	Uniformity of cell irradiation (percentage) 60-mm dish	100-mm dish	Array of 3 60-mm dishes
9	10	15.3	71.6	92.5	NA	NA
10	11	16.3	62.7	92.5	NA	NA
11	12	17.3	55.4	92.5	NA	NA
12	13	18.3	49.4	92.5	NA	NA
13	14	19.3	44.2	95	NA	NA
14	15	20.3	39.7	95	NA	NA
15	16	21.3	36.0	95	90	NA
16	17	22.3	32.7	95	90	NA
17	18	23.3	29.9	95	90	NA
18	19	24.3	27.4	95	90	NA
19	20	25.3	25.1	95	90	NA
20	21	26.3	23.2	95	92.5	NA
21	22	27.3	21.5	95	92.5	NA
22	23	28.3	20.0	95	92.5	NA
23	24	29.3	18.5	95	92.5	NA
24	25	30.3	17.3	95	92.5	NA
25	26	31.3	16.2	95	92.5	NA
26	27	32.3	15.2	95	92.5	90
27	28	33.3	14.2	95	92.5	90
28	29	34.3	13.4	95	92.5	90
29	30	35.3	12.6	95	95	90
30	31	36.3	11.9	95	95	90
31	32	37.3	11.2	95	95	90
32	33	38.3	10.6	95	95	90
33	34	39.3	10.1	95	95	90
34	35	40.3	9.5	95	95	92.5
35	36	41.3	9.1	95	95	92.5
36	37	42.3	8.6	95	95	92.5
37	NA	43.3	8.21	95	95	95

Table 6. Dose Rate Chart of 0.012-mm Al Beam

Hole # Room temp	Hole # Ice water	Shelf height SDD (cm)	Dose rate (cGy/s)	Uniformity of cell irradiation (percentage) 60-mm dish	100-mm dish	Array of 3 60-mm dishes
9	10	15.3	293	90	NA	NA
10	11	16.3	255	92.5	NA	NA
11	12	17.3	224	92.5	NA	NA
12	13	18.3	198	92.5	NA	NA
13	14	19.3	176	95	NA	NA
14	15	20.3	158	95	NA	NA
15	16	21.3	142	95	90	NA
16	17	22.3	128	95	90	NA
17	18	23.3	117	95	90	NA
18	19	24.3	106	95	90	NA
19	20	25.3	97.4	95	92.5	NA
20	21	26.3	89.5	95	92.5	NA
21	22	27.3	82.5	95	92.5	NA
22	23	28.3	76.2	95	92.5	NA
23	24	29.3	70.6	95	92.5	NA
24	25	30.3	65.6	95	92.5	NA
25	26	31.3	61.1	95	92.5	90
26	27	32.3	57.0	95	92.5	90
27	28	33.3	53.4	95	95	90
28	29	34.3	50.0	95	95	90
29	30	35.3	47.0	95	95	90
30	31	36.3	44.1	95	95	90
31	32	37.3	41.6	95	95	90
32	33	38.3	39.3	95	95	92.5
33	34	39.3	37.1	95	95	92.5
34	35	40.3	35.1	95	95	92.5
35	36	41.3	33.3	95	95	92.5
36	37	42.3	31.6	95	95	92.5
37	NA	43.3	NA	95	95	92.5

up to 0.5 ml of medium before irradiation. Notice that a shielding effect was present with as little as 0.1 ml of medium added to the dish. A similar effect was present for the triple-dish array.

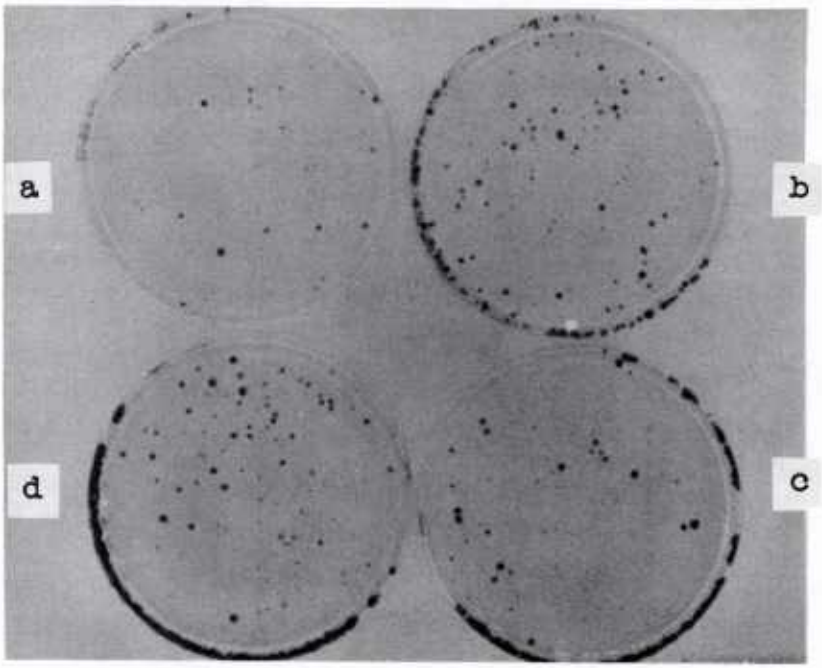

Figure 12. Meniscus effect for essentially unfiltered (0.012 mm Al) beam. The cell cultures were aspirated to completeness with increasing amounts of culture fluid added: (a) O ml, (b) 0.1 ml, (c) 0.3 ml, and (d) 0.5 ml.

SUMMARY

Dosimetry measurements have been performed on the AFRRI laboratory x-ray irradiator for three different cell culture dish arrays positioned at a range of distances from the x-ray tube. The device used for these measurements was a parallel-plate ionization chamber with a thin aluminized-mylar window. Intercomparison with an extrapolation chamber showed excellent agreement between these independent measurement methods. Results are presented for radiation dose rate, uniformity, and beam quality for operation of the tungsten target, Be window x-ray tube at 50 kVp, 20 mA, and with filters either 0.012 mm, 0.180 mm, or 0.633 mm thick. The data in this report establish a dosimetric link between the cellular radiobiology research to be performed at AFRRI with the laboratory x-ray irradiator and the landmark work performed by Elkind and Sutton (1) with a similar device.

REFERENCES

1. Elkind, M. M., and Sutton, H. Radiation response of mammalian cells grown in culture. Radiation Research 13: 556-593, 1960.

2. Christensen, E. E., Curray III, T. S., Dowdey, J. E. An Introduction to the Physics of Diagnostic Radiology. Lea and Febiger Pub., Philadelphia, 1978.

3. Personal communications with M. M. Elkind, June 1986.

4. Report of Calibration. DG 8454/85, TFNG45095. National Bureau of Standards, Gaithersburg, MD, 30 October 1985.

5. Seelentag, W. W., Panzer, W., Drexler, G., Platz, L., and Santner, F. A catalogue of spectra for the calibration of dosimeters. GSF-KBericht S 560. Gesellschaft fur Strahlen-und Umweltforschung mbH, Munich, Federal Republic of Germany, 1979.

6. Radiation Dosimetry, 2nd Ed. Vol. II: Instrumentation. Attix, F., and Roesch, C., eds. Academic Press, New York, 1966.

7. Johns, H. E., and Cunningham, J. R. The Physics of Radiology, 4th ed. C. Thomas Pub., Springfield, IL, 1983.

8. Trout, E. D., Kelly, J. P., and Lucas, A. C. Determination of half value layer, American Journal of Roentgenology 84: 729-740, 1960.

ACKNOWLEDGMENTS

The authors would like to thank Dr. Colin K. Hill for his helpful discussions and advice in planning this project. We would like to especially thank Mr. Franklin M. Sharpnack for the construction of the petri dish holders and acrylic positioning devices for the x-ray irradiator. We would also like to thank Mr. Scott Hawkins for the copious dosimetry measurements he made, which are included in this report. Finally, we acknowledge and thank Dr. Michael P. Hagan for his invaluable assistance and guidance in numerous aspects of this project.

APPENDIX A. X-RAY ENERGY SPECTRA

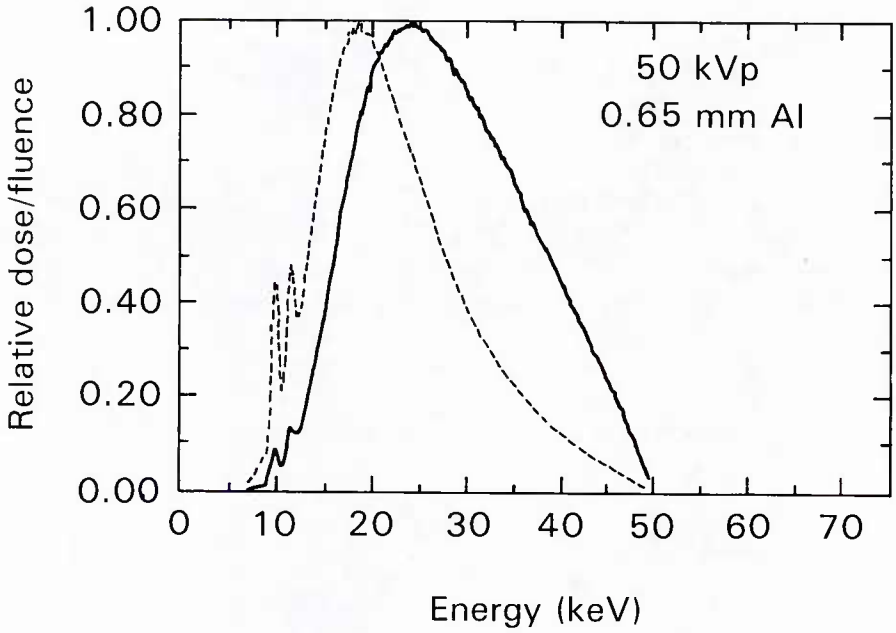

Figure A-1. X-ray energy spectrum for 50 kVp and 0.65 mm Al filtration. The solid line shows the spectral distribution of x-ray energy, and the dash line shows that of x-ray fluence. Redrawn from reference (5).

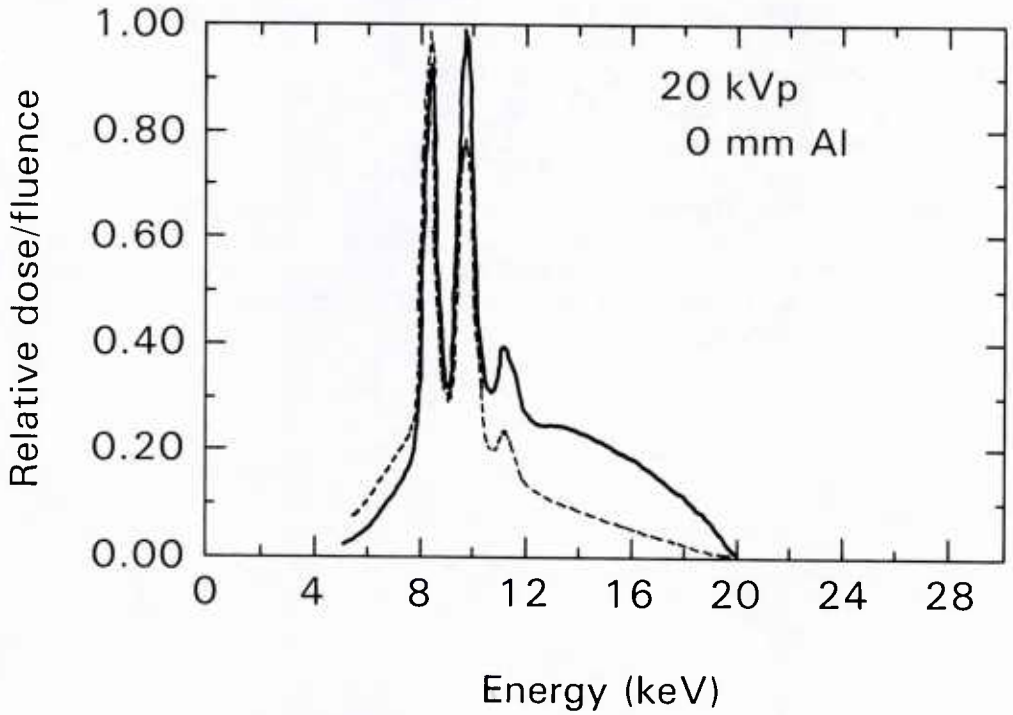

Figure A-2. X-ray energy spectrum for 20 kVp and no added filtration. The solid line shows the spectral distribution of x-ray energy, and the dash line shows that of x-ray fluence. Redrawn from reference (5).

APPENDIX B. EXPOSURE AND DOSE CALCULATIONS FOR THE PARALLEL-PLATE IONIZATION CHAMBER

$$\dot{X} = (\Delta Q/\Delta t)\ N_x\ k_{tp} \qquad \text{(B-1)}$$

where $\dot{X}$ = exposure rate in R/s

ΔQ = charge collected over time interval Δt (nC/s)

N_x = chamber calibration factor (see table 1). The calibration factor whose HVL and homogeneity factor most closely resembles the values measured for each field was chosen for that field. The uncertainty in applying this method is approximately 1%.

= 6.502 R/nC for 0.633 mm added Al beam

= 6.349 R/nC for 0.180 mm added Al beam

= 6.348 R/nC for 0.012 mm added Al beam

k_{tp} = correction to standard room temperature and pressure

$$\dot{D} = \dot{X}\ f_{water}\ k_{bs}\ k_{sw} \qquad \text{(B-2)}$$

where $\dot{D}$ = absorbed dose rate to cell medium (cGy/s)

f_{water} = factor that converts exposure in air to dose in water, which approximates the cell media. This is an energy dependent value, although it varies less than 2.5% over the equivalent energy ranges involved (7).

= 0.886 for 0.633 mm added Al beam

= 0.902 for 0.180 mm added Al beam

= 0.905 for 0.012 mm added Al beam

k_{bs} = correction for backscatter. This correction was assumed to be 1.00 because the amount of plastic behind the ionization chamber was approximately the same as behind the cells.

k_{sw} = correction for attenuation due to plastic wrap. This correction was only applied to the 0.633 mm Al beam. Plastic wrap was included in the measurements of the other fields.

= 1.02 for 0.633 mm added Al beam

APPENDIX C. DERIVATION OF EXPOSURE RATE CALCULATION FOR EXRAPOLATION CHAMBER (3)

a. Definition of Exposure:

1 R in dry air for x or γ rays = 1 esu charge / cm^3 at STP

$\therefore$ 1 R = 3.336×10^{-10} C/cm^3

b. Conversion of C/cm^3 to amp-s/cm^3 at STP

Given: 1 amp = 1 C/s

1 C = 1 amp-s

$\therefore$ 1 R = 3.336×10^{-10} amp-s/cm^3

and 1 R/s = 3.336×10^{-10} amp/cm^3

c. Define:

$$K = \frac{1 \text{ R/s}}{3.336 \times 10^{-10}} = 2.998 \times 10^{9} \left[(\text{R/s})/(\text{amp/cm}^3)\right]$$

d. $$\dot{X} = \frac{K \, dQ/dt}{V_{STP}} = K \left[\frac{\text{R/s}}{\text{amp/cm}^3}\right] \frac{I \text{ (amp)}}{V_{STP} \text{ (cm}^3\text{)}}$$

$$= 2.998 \times 10^{9} \, (I/V_{STP})$$

where I = current of charge generated in air volume V at STP conditions

e. Volume of a right circular cylinder (V) = $\pi r^2 h$
where r is the radius and h is the height
Correct the air volume to room temperature and standard pressure.

$$V_{STP} = \left[\frac{295.15}{T + 273.15}\right] \left[\frac{P}{760}\right] (\pi r^2 h)$$

where T is the air temperature in ^{o}C and P is the atmospheric pressure in mm of mercury.

f. $$\dot{X} = 2.457 \times 10^{9} \left[\frac{T + 273.15}{P}\right] \left[\frac{I_c}{r^2 h}\right] \quad (C\text{-}1)$$

where r = the extrapolation effective radius (cm)
I_c/h = slope of line from chamber response (amp) vs. separation of window-anode (cm)
h = separation distance of the extrapolation chamber window from the anode